

OPERATING CONDITIONS FOR BIG BUBBLE CHAMBERS (15' CHAMBER)
FILLED WITH NEON/HYDROGEN MIXTURES

Gert G. Harigel

June 16, 1974

It is the purpose of the present note to make a few general remarks on track quality in big chambers, to give a review of operating conditions for pure liquids (hydrogen and neon), as well as provide a comparison of the results in neon/hydrogen mixtures with those in pure liquids. It is our further intention to propose operating temperature and pressure for a 20/80 mole percent neon/hydrogen mixture, and finally to make technical remarks concerning the measurement of the dynamic pressure, neon concentration, and phase separation.

1. TRACK QUALITY IN BIG CHAMBERS

The following five points will provide a basis for a better understanding of this technical note and should be kept in mind when judging our conclusions.

1.1 Extrapolation of results from medium-sized chambers

Systematic investigations of bubble growth and density were made in the 85 cm cryogenic bubble chamber at DESY ⁽¹⁾ under the following conditions:

- (1) using bright field illumination with a 1 : 1 demagnification optic,
- (2) particle injection only in the pressure minimum of the expansion cycle (the dynamic pressure was measured with two piezo-electric transducers, one close to the piston region, the other - close to the beam plane, results obtained only with the latter are considered in the present note),
- (3) one cycle duration for the piston movement (≤ 30 ms, pressure P_{static} to P_{static} ca. 22 ms) because of the chamber's resonance expansion system. Fig.1 gives a typical pressure versus time curve from this experiment. Note, that similar to the piston stroke curve, the pressure curve is asymmetric to the pressure minimum! There is a steeper gradient of the pressure during recompression than during expansion. This asymmetry seems to increase with increasing neon concentration. It may be due to the change in sound velocity and to the increase of the hydrostatic pressure. Studies, comparing piston stroke and pressure versus time dependencies, are in progress.

Note (as a rule of thumb, no satisfactory theoretical explanation is available) that bubble sizes start to diminish, when during recompression the dynamic pressure reaches the limit of sensitivity. For all experiments in pure hydrogen the corresponding flash delay time was $8 \div 10$ ms, for pure neon $5 \div 7$ ms, and for the mixtures -

somewhere between these limits. The bubble growth constant A was determined from diameters of bubbles photographed with flash delays up to 5 ms, no corrections for pressure variations were applied.

The volume change necessary during expansion to obtain a certain pressure drop, is always larger than expected from the value of the compressibility of the liquid. This difference is proportional to the irreversible heat (parasitic boiling) and should become smaller with increasing volume-to-surface ratio for larger bubble chambers.

In big chambers, the length and shape of the expansion cycle can either be completely adjusted to the characteristics of the liquids to be used (BEBC), or can at least be increased to some degree by changing the natural frequency of the resonator and the spring constant of the driving motor (15' chamber). Furthermore, particles can be injected a few milliseconds before the pressure minimum. Both modifications will favor an increased bubble growth rate compared with data taken from (1). In order to keep flash delays short and, consequently, systematic and random track distortions small, such an increase is particularly desirable for big chambers.

However, the possible gain in growth rate in big chambers compared with that in small chambers is not yet well known and therefore it is not considered in the present note. We limit ourselves to a comparison of the results in pure liquids and mixtures obtained from a medium-sized chamber under similar conditions.

1.2 Ionization information

In big chambers even at high energies of the primary particles the measurement of bubble density, gap or blob length distribution will be of aid to determine the particle mass of the slower secondary particles. The choice of the bubble density for minimum ionizing particles will probably be restricted to $b \approx 5 \div 10 \text{ cm}^{-1}$; this range is determined by the optical demagnification and by bubbles, which must be of certain size.

.3 Uniform track quality in the fiducial volume

Bubble sizes and densities should be identical everywhere in the fiducial volume, or at least not smaller on the bottom than on the top of the chamber. Uniform expanded pressure throughout the liquid volume during the time interval between particle injection and photography is necessary. Low sound velocity and hydrostatic pressure of the heavier liquids act against it.

A request was made to find conditions for mixtures, where the track quality approaches the one obtained in hydrogen (deuterium). If possible, growth times should be smaller than ca. 10 ms.

1.4 No optimization for a simultaneous operation of a track sensitive target

No request was made here to optimize the track quality simultaneously in a mixture of neon/hydrogen and in a hydrogen or deuterium-filled passive or active track sensitive target. The proposed working conditions would then be altered according to neon concentration.

1.5 Bubble movement

The movement of bubbles ⁽²⁾ is mainly due to gravity forces, displacement of the liquid during its expansion or recompression, and to inertia forces. These systematic displacements can be measured and corrections can be made, at least in principle, during the reconstruction in space. Due to small eddies in the liquid, random bubble movement can and does occur and is superimposed upon the systematic bubble displacement.

Both, systematic and random displacements, depend upon liquid temperature, dynamic pressure, piston speed, chamber geometry, as well as upon the time of particle injection and the photography of the bubble tracks.

The above displacements and their influence upon momentum and the determination of the angle should be small also for big chambers.

This can be achieved by operating large chambers at low temperatures, provided that the parasitic boiling around the piston region on the bottom of the chamber can be also kept at a minimum.

2. WORKING CONDITIONS FOR PURE HYDROGEN

2.1 Bubble densities b [cm^{-1}] and growth rates A [$\text{cm}/\text{s}^{\frac{1}{2}}$]

The above two quantities are given in fig.2 as a function of the expanded pressure P_{min} [bar] (particle injection at the dynamic pressure minimum) for a wide range of liquid temperatures T in a PT-diagram. "A" is the proportional constant from the well known $R = A \cdot \sqrt{t}$ - law, where R is the radius of the bubble [cm] at the flash delay time t [s]. Example: for optical reasons a bubble diameter of 0.7 mm (typical for our big chambers) is necessary and at a chosen temperature and expanded pressure the proportional constant is $A = 0.4 \text{ cm}/\text{s}^{\frac{1}{2}}$; the required flash delay will then be ca. 8 ms during which a bubble grows to the above size.

Fig.2 also indicates the dependency of the vapor pressure and that of the limit of sensitivity (bubble density is close to $b = 0 \text{ cm}^{-1}$, but increases with increasing pressure drop) upon temperature.

For all practical applications the presentation of our results in a temperature versus expanded pressure diagram is helpful. To obtain curves of constant bubble density and growth rate some interpolations between our results given elsewhere ⁽¹⁾ as a function of the expanded pressure, are necessary.

Note, that for a given bubble density higher growth rates can be achieved by decreasing the liquid temperature.

2.2 Sound velocity c [m/s]

In hydrogen the sound velocity is high and varies slightly within the range of the most likely operating temperatures of bubble chambers (25 ÷ 29 K) ⁽³⁾, cf. fig.3. It takes ca. 4 ms for a sound wave in the 15' chamber to travel from the piston region to its top. If we consider only the height of the fiducial volume (ca. 2 m), then within 2 ms similar expanded pressures can be achieved in this region. This presents no serious limitations for having similar track quality, as long as the particle injection is close to the pressure minimum and the total cycle duration is not much shorter than $L \approx 50$ ms. The latter conditions maintain the absolute value of the pressure-time gradient small during the bubble growth period.

2.3 Radiation length X^0 [cm]

The radiation length depends upon the atomic number and the density of the material. In hydrogen the density of the liquid ρ_L varies little with temperature (0.0647 g/cm³ at 25 K, and 0.0569 g/cm³ at 29 K). The radiation length is ca. 900 cm which, even in big bubble chambers, is just too high to provide a reasonable gamma-conversion probability.

2.4 Bubble movement

A detailed study of the movement of bubbles was conducted in the DESY chamber ⁽²⁾ and its results are applicable to big chambers as well.

2.5 Vapor pressure P_v [bar] and compressibility β [bar⁻¹]

For hydrogen, the temperature dependency of these two quantities has been established ^{(3), (4)}. Without creating technical problems, they allow for a large range of operating conditions.

3. WORKING CONDITIONS FOR PURE NEON

3.1 Bubble densities b [cm^{-1}] and growth rates A [$\text{cm/s}^{\frac{1}{2}}$]

These two quantities are given in fig.4 as a function of temperature when particle injection is at the pressure minimum ⁽¹⁾. The measurements were performed only in a restricted range of relatively low temperatures due to the technical limitations of the cooling system of the DESY chamber. For high-energy physics experiments bubble densities at this temperature are obviously unsatisfactory. In spite of the very poor data obtained, the results are extrapolated to higher temperatures (dotted/dashed lines). At $T = 36$ K, $P_{\text{min}} = 3.5$ bar, a better track quality with the density $b = 10 \text{ cm}^{-1}$ and a growth factor $A = 0.4 \text{ cm/s}^{\frac{1}{2}}$ is expected.

The thermal conductivity of pure hydrogen and neon is nearly identical at $T = 26.5$ K ($k = 1.33 \cdot 10^{-3}$ W/cm K for hydrogen, and $k = 1.44 \cdot 10^{-3}$ W/cm K for neon), but then drastically drops with increasing temperature for neon at $T = 36$ K by one order of magnitude.

3.2 Sound velocity c [m/s]

Measurements in neon ⁽³⁾ are available between $T = 25 \div 31$ K, and an extrapolation of these data to the temperature of $T = 36$ K gives $c \approx 410$ m/s (fig.5). For hydrogen this value is about double at $T = 25.3$ K. To compensate for this drawback and to get similar track quality throughout the liquid volume, the duration of the expansion cycle for neon should be double the one for hydrogen.

3.3 Radiation length X° [cm]

The radiation length in neon is $X^{\circ} = 27$ cm (ca. 1/30 of the one in pure hydrogen) and it changes little with liquid density ($\rho_L = 1.07$ g/cm³ at $T = 34$ K, $\rho_L = 1.00$ g/cm³ at $T = 37$ K). For comparison: X° (propane C₃H₈) = 110 cm, X° (freon CF₃Br) = 11 cm, which are the most common liquids for "heavy liquid bubble chambers."

3.4 Bubble movement

It will certainly be of interest to study bubble movement photographed in the DESY chamber ⁽¹⁾. It is expected to be quite different from pure hydrogen. The lift velocities v [cm] in the two liquids can be calculated from the theory

$$v = \sqrt[5]{\frac{4 \cdot \rho_v \cdot \sigma^2 \cdot g}{12 \cdot \pi \cdot \rho_L^2 \cdot \eta}}$$

using the well known values for the densities of the gas in the bubble ρ_v [g/cm³] and the liquid ρ_L [g/cm³]; the viscosity η [g/cm·s] (fig.7), and the surface tension σ [g/s²] (fig.8). This gives

$$v(\text{H}_2, 25 \text{ K}) = 1.8 \cdot v(\text{Ne}, 36 \text{ K}) .$$

3.5 Vapor pressure P_v [bar] and compressibility β [bar⁻¹]

Numerical values for both properties in neon differ considerably from those in hydrogen. The temperature range for the operation of present-day cryogenic bubble chambers with pure neon is much smaller than in hydrogen: the sensitivity to ionizing particles (degree of overheat which can be achieved) determines its lower limit to ca. 34.5 K; its upper limit is given by the design pressure of the chamber body. If we allow for a maximum pressure of 10 bar, the highest vapor pressure of the liquid may be $P_v = 9$ bar, i.e. $T = 37$ K.

The isentropic compressibility of neon is given in fig.6. Between 25 and 31 K it is calculated from the measurements of the sound velocity and density of the liquid $\beta = 1/\rho_L \cdot c^2$ ⁽³⁾; at temperatures 34.5 and 34.9 K it is determined from pressure-volume diagrams derived from bubble chamber expansions ⁽⁵⁾.

The operation of a chamber with neon at 36 K is quite similar to hydrogen at 25.3 K, as far as bubble densities and growth rates are concerned. However, the compressibilities of the two liquids are quite different: $\beta = (0.60 \pm 0.05) \cdot 10^{-3}$ bar⁻¹ for neon and $1.8 \cdot 10^{-3}$ bar⁻¹ for hydrogen. The total pressure drop will be $\Delta P \lesssim 5.3$ bar for neon, but

only 3.1 bar for hydrogen, assuming 1 bar overpressure in each case. An expansion ratio of $\Delta V/V = 0.75\%$ was measured in hydrogen, and with a reasonable safety margin we can estimate a ratio of $\Delta V/V \lesssim 0.5$ in neon.

The practical consequences for existing resonance-type chambers are:

- (1) in pure neon there are no problems with the piston stroke, but difficulties can arise with pressure overshoots and oscillations after recompression, which may be as high as 50 % of the total pressure drop during expansion, thereby increasing the acceleration forces. These overshoots can be partially avoided in the 15' chamber by adjusting correctly the latch pressure.
- (2) An operation of the chamber's heat exchangers with hydrogen is excluded in the entire temperature range (critical point of hydrogen: $P_c = 12.8$ bar, $T_c = 33.2$ K), the operation with deuterium is feasible but probably difficult due to the high vapor pressure of this liquid ($P_v = 10.4 \div 13.7$ bar at $T = 35 \div 37$ K). The easiest and cheapest solution may be to use pure neon.

One may recommend, therefore, that the vapor pressure be reduced in big bubble chambers and the liquid be "softened" by adding some hydrogen or - even better - deuterium to the neon filling. A detailed discussion of the operating conditions of these mixtures is, however, beyond the scope of the present note.

4. WORKING CONDITIONS FOR NEON/HYDROGEN MIXTURES WITH LOW NEON CONCENTRATIONS

4.1 Operating temperature T [K]

There are two limits for the operating temperature of neon/hydrogen mixtures. They are extracted from the work of Street and Jones ⁽⁶⁾ and are shown in a temperature-concentration diagram (fig.9). The neon/hydrogen concentration is given throughout our paper in mole percent, its relation with atomic and weight percent is shown in fig.10. The lower operation limit is reached at phase separation the upper - at the admissible vapor and static pressure, the latter should not exceed the design pressure of the chamber body. Systematic measurements of the bubble density and growth were performed in the DESY chamber under stable conditions, indicated as points in fig.9.

Reasons exist for not operating a bubble chamber too close to these limits:

- (1) The first being the adiabatic temperature drop in the liquid during expansion (values have to be determined by interpolating the results in the two pure liquids: $\Delta T_{ad} \approx 0.1$ K/bar for hydrogen, $\Delta T_{ad} \approx 0.01$ K/bar for neon). This temperature drop throughout the entire liquid may result in a complete phase separation inspite of the short duration of the expansion cycle. Attention should be paid to the subcooled layer of the liquid around the bubble: here, the chances for phase separation are even higher than throughout the entire liquid, but only a very limited fraction of it is involved.
- 2) The second reason is that in resonant type bubble chambers the pressure oscillations after recompression, originating from the low compressibility of the mixture, may become too high: their peak value should be kept smaller than 10 bar.

Taking both considerations into account, leaves us with a rather all temperature interval (hatched zone in fig.9) for a stable

operation of neon/hydrogen filled chambers.

Tables 1 and 2 give the measured liquid densities ρ_L [g/cm^3] and sound velocities c [m/s] as a function of temperature T for this interval.

4.2 Bubble densities b [cm^{-1}] and growth rates A [$\text{cm/s}^{1/2}$]

Results of the measurements of bubble densities b and growth rates A in neon/hydrogen mixtures can be compared with those at various identical temperatures in pure hydrogen. Such an examination shows:

- (1) Bubble creation and growth process is essentially governed by the hydrogen component of the mixture, at least up to 55 mole percent neon concentration. When measured at 83.8 mole percent neon concentration, considerable deviations from the above behavior were observed. Compare fig.2 with figs. 11 and 12.
- (2) Bubbles stop growing earlier in mixtures than in pure hydrogen, as was discovered in a resonant-type expansion bubble chamber.
- (3) In big chambers hydrostatic pressure increases considerably from the top of the chamber towards the piston region. This may further reduce in the mixtures the already slow growth rate, as well as the bubble density near the bottom of the chamber.
- (4) Since bubble growth rates are small, recompression times are long: already shown in the first paper on the use of mixtures in bubble chambers ⁽⁸⁾, it was confirmed during experiment ⁽¹⁾. To accelerate the recompression (recondensation) process, high overpressures $P_{\text{over}} > 1 \text{ bar}$ are desirable.
- (5) Some additional values for bubble densities at high neon concentrations can be found in ⁽⁹⁾, demonstrating the limitations of neon/hydrogen mixtures in combination with track sensitive deuterium target.

4.3 Compressibility β [bar^{-1}] and expansion ratio $\Delta V/V$ [%]

The required pressure drop to achieve equivalent sensitivity in hydrogen is the same as in neon/hydrogen mixtures up to about 55 mole percent neon concentration. Above 55 mole percent, all operating conditions differ from those in pure hydrogen and in pure neon, the pressure drop especially will differ considerably from the one in pure hydrogen. Compare figs.2 and 4 with figs.11, 12, 13, 14, 15, and 16.

The expansion ratios for all pressure drops used during the DESY experiments with hydrogen, neon, and the neon/hydrogen mixtures are summarized in table 3. A comparison of these expansion ratios with those used in the Brookhaven 20-in. bubble chamber ⁽⁸⁾, using the same temperatures and expanded pressures, show similar behavior, but only in the DESY chamber expanded pressures were always obtained with a smaller expansion ratio. There are several reasons: there is less parasitic boiling in the chamber, the piston region in the DESY chamber is better cooled, and there is better tightness of the piston rings. A comparison of our results with those obtained from the Rutherford 1.5 m bubble chamber gives no additional information since in the latter case a gas expansion system is used.

The expansion ratios for low neon concentrations do not differ much from those in pure hydrogen, but become significantly smaller with increasing neon concentration (cf. table 3). High pressure drops can then be achieved with small piston strokes, such pressure drops are obviously related to the compressibilities of the mixtures. Table 3 includes very preliminary values for isentropic compressibilities, determined from pressure-volume diagrams taken during our experiment. A more detailed discussion of these values, all of which seem to be higher by several percent than those given in ⁽³⁾, is in preparation ⁽⁵⁾. The values of ⁽³⁾ are reproduced in fig.17, which in addition includes a curve which connects temperature and concentration values, at which the Brookhaven 20-in. chamber was operated. This diagram is complemented by a curve, which presents our proposed operating conditions for big chambers.

4.4 Bubble movement

This process has not been studied in mixtures so far. It is expected to be different from hydrogen due to different liquid densities ρ_L , viscosities η , and surface tension σ , the latter two being yet insufficiently accurate to obtain theoretical calculations. However, bubble movement can be determined if we use the film from experiment ⁽¹⁾.

4.5 A 20/80 mole percent neon/hydrogen mixture

Enough neon may soon be purified at FNAL to fill the 15' bubble chamber with a 20/80 mole percent neon/hydrogen mixture. The radiation length for this relatively low neon concentration is about 200 cm, i.e. ca. 1/5 of pure hydrogen (cf. fig.18). This mixture may not be insofar of any particular interest for high-energy physics, but it will certainly complement initial results obtained with a 34/66 mole percent neon/hydrogen mixture in the 12' chamber at Argonne ⁽¹⁰⁾. It will also give relevant information on the use of neon/hydrogen mixtures in large piston-expanded chambers. Furthermore, it may provide a better idea about anticipated working conditions at very high neon concentrations. Note especially, that for 97/3 mole percent neon/hydrogen, the sound velocity is about the same as in the low 20/80 mole percent mixture (cf. table 2).

Two sets of measurements of bubble density and growth rate in the vicinity of 20/80 mole percent neon/hydrogen mixture are available: one, obtained from explorative measurements of bubble densities in a 15/85 mole percent neon/hydrogen mixture ⁽⁷⁾; the second - from a 31.9/69.1 mole percent neon/hydrogen mixture ⁽¹⁾, which gives precise results for bubble densities up to high values, but comprises only low growth rates. Bearing the conclusions of paragraph 4.2 in mind, we are allowed to interpolate the results in pure hydrogen and the 31.9/68.1 mole percent neon/hydrogen mixture, to find the operating conditions for a 20/80 mole percent neon/hydrogen mixture.

In recent test runs, the 15' chamber at FNAL and the 7' chamber in BNL were operated successfully with pure hydrogen at $T = 25.3$ K and $P_{\min} \approx 1.4$ bar without problems. Therefore, it will be even easier to expand the 15' chamber to $P_{\min} = 1.6$ bar. Using fig.2, we find for the above pressure and temperature a bubble density of $b \approx 10$ cm⁻¹ and a growth constant $A \approx 0.4$ cm/s^{1/2}, i.e. ideal conditions for fast growth, short flash delay and little track distortions.

Unfortunately, at 25.3 K the 20/80 mole percent neon/hydrogen mixture can not be operated without consequences, since the above temperature approaches the limit of phase separation (cf. fig.11 and extrapolate the curves to 25.3 K).

The operation of the above mixture even at 26.0 K is still somewhat of a problem, if one takes into account that the heat exchangers around the piston should be kept ca. 1 K colder than the mean liquid temperature. This will cool the liquid around the heat exchangers more than is acceptable; then too, there is a further subcooling due to the adiabatic temperature drop during the expansion. A fall-out of solid neon was observed at 23.8 K ⁽⁷⁾, neon has its triple point at $T_t = 24.56$ K and $P_t = 0.43$ bar.

A more stable operating temperature would therefore be $T = 26.5$ K. However, compromises have to be made then either with bubble density, which will be higher than $b = 10$ cm⁻¹, but with the growth rate being still $A = 0.4$ cm/s^{1/2}; or one must sacrifice the growth rate, which will be lower than is desirable, but bubble density will be at a value which still allows for ionization measurements. The main parameters for the two alternative conditions are summarized in table 4.

For a 20/80 mole percent neon/hydrogen mixture at $T = 26.5$ K the isentropic compressibility is only about 10 percent higher than in pure hydrogen at $T = 25.3$ K (cf. fig.17), and, consequently, the expansion ratios will be approximately the same for identical pressure drop. The sound velocities are $\bar{c} = 955$ and 645 m/s, resp. To obtain the same pressure distribution in the liquid, the cycle duration must be

increased from $L = 55$ ms in hydrogen to $L = 80$ ms in the mixture. This is feasible by retuning the expansion system in the 15' chamber. The densities of the two liquids differ by $\rho_L(20/80 \% \text{ Ne/H}_2) / \rho_L(100/0 \% \text{ Ne/H}_2) \approx 3.4$.

The condition (2) in table 4 (i.e. 20/80 mole percent neon/hydrogen at $P_{\text{min}} = 2.8$ bar) simulates closely the operation of the chamber with 97/3 mole percent neon/hydrogen mixture at $T = 31.5$ K for sound velocity, bubble growth and density, whereas the liquid density

$\rho_L(20/80 \% \text{ Ne/H}_2) / \rho_L(97/3 \% \text{ Ne/H}_2) \approx 0.18$ and its compressibility $\beta(20/80 \% \text{ Ne/H}_2) / \beta(97/3 \% \text{ Ne/H}_2) \approx 5.0 \pm 0.5$; the radiation length $X^0(20/80 \% \text{ Ne/H}_2) / X^0(97/3 \% \text{ Ne/H}_2) \approx 7$.

5. TECHNICAL PROBLEMS DUE TO PHASE SEPARATION OF MIXTURES

Changes in the mixture composition will always occur during a bubble chamber run, resulting in a higher neon concentration on the bottom than on the top of the chamber. This gradient is caused by the phase separation on the surface layer of all bubbles and is correlated with their movement due to gravity. A chance for phase separation on the surface of the heat exchangers, which are by ca. 1 K colder than the bulk liquid, is probable. For all high-energy physics experiments it is necessary to determine the degree of separation:

- (1) one can take gas probes through thin pipes on the top and on the bottom of the chamber in regular sequences and analyze them as quickly as possible,
- (2) one can measure the density of the liquid throughout the chamber either by a method used in the 80" chamber in BNL ⁽¹¹⁾, or by sonic probes where the vapor pressure thermometers are located at the top and the bottom of the chamber.
- (3) one can measure the density of the liquid indirectly with the range of particles coming to rest ⁽¹²⁾, a time-consuming method, which has to be investigated further in the 15' chamber, since beam particles with low energy are necessary.

Some means must be found to circulate the liquid inside the chamber in order to improve its homogeneity.

Unknown factors, arising from the chamber geometry require a determination of the dynamic pressure in various regions of the chamber. Pressure variations throughout the liquid are almost unpredictable at this stage.

The ultimate reconstruction accuracy of events certainly depends upon the duration of the expansion-recompression cycle. This problem can be treated only experimentally. It should be investigated whether the change in bouncer mass and gasspring ratio is sufficient to adapt to the desired cycle duration for the liquid characteristics in the 15' bubble chamber.

6. ACKNOWLEDGEMENT

I would like to thank the 15' bubble chamber group for the warm hospitality extended to me; my special thanks go to Dr. F.R. Huson for arranging my visit to the Fermi National Accelerator Laboratory and to Dr. W.B. Fowler for initiating the present study.

7. REFERENCES

- (1) G. Horlitz, S. Wolff,
G. Harigel Bubble Growth and Bubble Densities
in Bubble Chambers Filled with Neon/
Hydrogen Mixtures,
DESY 73/41, (1973) and
Nucl.Instr.Meth. 117, 115, (1974)
- (2) G. Harigel, G. Horlitz,
S. Wolff On the Movement of Bubbles in a
Medium-Sized Bubble Chamber,
DESY 72/16, (1972)
- (3) D. Güsewell, F. Schmeissner,
J. Schmid New Data on Liquid Neon-Hydrogen
Mixtures,
Cryogenics, August (1971), 311
- (4) G. Horlitz, S. Wolff,
G. Harigel On the Thermodynamics of Bubble
Chamber Expansions,
DESY 68/43, (1968)
- (5) G. Harigel, G. Horlitz,
S. Wolff On the Thermodynamics of Bubble
Chamber Expansions in Liquid
Neon/Hydrogen Mixtures,
(in preparation)
- (6) W.B. Street, C.H. Jones Liquid Phase Separation and Liquid-
Vapour Equilibrium in the System
Neon-Hydrogen,
Journal Chem.Phys. 42, 3989, (1965)
- (7) R. Florent, C. Geles,
G. Harigel, H. Leutz,
F. Schmeissner,
J. Tischhauser, G. Horlitz,
S. Wolff, H. Filthuth Operation of a Track Sensitive
Hydrogen Target Inside a Neon-
Hydrogen Bubble Chamber,
Nucl.Instr.Meth. 56, 160, (1967)
- (8) R.C. Albert, C.L. Goodzeit,
F.C. Pechar, A.G. Prodehl Neon-Hydrogen Bubble Chambers,
Adv. Cryogenic Eng. 11, 321, (1965)
- (9) G. Horlitz, S. Wolff,
G. Harigel, H. Leutz,
F. Schmeissner Operation of a Track Sensitive
Deuterium Target Inside a Neon-
Hydrogen Bubble Chamber,
Nucl.Instr.Meth. 68, 312, (1969)
- (10) K. Jaeger private communication
- (11) J. Sondericker private communication
- (12) J.G.V. Guy, J.W.G. Wignall,
C.M. Fisher A Study of the Variation of the
Neon Concentration during an Ex-
periment with a Track Sensitive
Target,
Rutherford Lab. RL-74-035, (1974)
- (13) J.E. Jensen, R.B. Stewart,
W.A. Tuttle Selected Cryogenic Data Notebook,
BNL 10200, (1966)

8. FIGURE CAPTIONS

- (1) Typical pressure-time curve for a neon/hydrogen mixture with high neon concentration in the resonant-type DESY bubble chamber.
- (2) Bubble densities b [cm^{-1}] and growth rates A [$\text{cm/s}^{1/2}$] for pure hydrogen in a pressure-temperature diagram ⁽¹⁾. T_c and P_c are the critical temperature and pressure, resp., where all curves for bubble densities should merge with the vapor pressure.
- (3) Sound velocity c [m/s] in normal liquid hydrogen as function of temperature ⁽³⁾, ⁽¹³⁾
- (4) Bubble densities b [cm^{-1}] and growth rates A [$\text{cm/s}^{1/2}$] for pure neon in a pressure-temperature diagram ⁽¹⁾. The limit of sensitivity was determined with low accuracy. Dashed/dotted lines are very crude extrapolations of the experimental data to higher temperatures. Bubble densities of $b = 2.5$ and 5 cm^{-1} are extrapolated from measured values at 34.9 K to lower and higher temperatures. The anticipated value for an operation with $b = 10 \text{ cm}^{-1}$ and $A = 0.4 \text{ cm/s}^{1/2}$ is indicated as a circle.
- (5) Sound velocity c [m/s] in liquid neon as a function of temperature. The dotted line is a rough extrapolation to higher liquid temperatures, using the known liquid density ⁽¹³⁾ and the measured compressibilities at 34.5 and 34.9 K ⁽⁵⁾.
- (6) Isentropic compressibilities β [bar^{-1}] of liquid neon as a function of temperature. The values at 34.5 and 34.9 K are determined from a bubble chamber experiment ⁽⁵⁾, using pressure-volume diagrams during expansion. The solid curve is taken from ⁽³⁾. The curve is further extrapolated to 36 K, giving a value $c \approx 0.6 \cdot 10^{-3} \text{ bar}^{-1}$.
- (7) Viscosity η [$\text{g/cm}\cdot\text{s}$] of liquid neon as a function of temperature ⁽¹³⁾

- (8) Surface tension σ [g/s^2] of liquid neon ⁽¹²⁾. The value at 36 K is determined by linear extrapolation of measured values.
- (9) Measurements of bubble growth and bubble density in the DESY chamber; points are given in a temperature-concentration diagram ⁽¹⁾. Indicated are the region of phase separation $\textcircled{1}$, the vapor pressures, and the region where bubble chamber operation is no longer possible $\textcircled{2}$, and the probable region of operation $\textcircled{3}$. Curves of constant vapor pressure P_v |bar| are extracted from ⁽⁶⁾.
- (10) Relation between mole percent, atomic and weight percent in neon/hydrogen mixtures.
- (11) Bubble densities b [cm^{-1}] and growth rates A [$\text{cm/s}^{\frac{1}{2}}$] in a pressure-temperature diagram for 31.9/68.1 mole percent neon/hydrogen mixture, measured at 28.0, 28.5, and 28.95 K ⁽¹⁾. The growth rate $A = 0.2 \text{ cm/s}^{\frac{1}{2}}$ was determined by extrapolation from lower values.
- (12) Bubble densities b [cm^{-1}] and growth rates A [$\text{cm/s}^{\frac{1}{2}}$] in a pressure-temperature diagram for 53.8/46.2 mole percent neon/hydrogen mixture, measured at 29.0 K ⁽¹⁾.
- (13) Bubble densities b [cm^{-1}] and growth rates A [$\text{cm/s}^{\frac{1}{2}}$] in a pressure-temperature diagram for 83.8/16.2 mole percent neon/hydrogen mixture, measured at 28.95 and 29.45 K ⁽¹⁾. This is the only mixture ratio, where bubble growth curves seem to have a steeper gradient than curves of constant bubble densities.
- (14) Bubble densities b [cm^{-1}] and growth rates A [$\text{cm/s}^{\frac{1}{2}}$] in a pressure-temperature diagram for 86.6/13.4 mole percent neon/hydrogen mixture, measured at 28.5 and 29.4 K ⁽¹⁾.
- (15) Bubble densities b [cm^{-1}] and growth rates A [$\text{cm/s}^{\frac{1}{2}}$] in a pressure-temperature diagram for 92.3/7.7 mole percent neon/hydrogen mixture, measured at 28.0, 29.5, and 30.0 K ⁽¹⁾. At 28.0 K the bubble density $b < 1 \text{ cm}^{-1}$.

- (16) Bubble densities b [cm^{-1}] and growth rates A [$\text{cm/s}^{1/2}$] in a pressure-temperature diagram for 96.7/3.3 mole percent neon/hydrogen mixture, measured at 31.0, and 32.0 K ⁽¹⁾. At 31.0 K and 1.5 bar is the bubble density $b < 3 \text{ cm}^{-1}$.
- (17) Isentropic compressibilities β [bar^{-1}] of saturated liquid neon/hydrogen mixtures in the temperature range $T = 25 \div 31 \text{ K}$, versus neon mole fraction. Solid lines are calculated from measured liquid densities ρ_L [g/cm^3] and sound velocities c [m/s], taken from ⁽³⁾ (cf. tables 1 and 2). The broken line indicates the operating concentrations and temperatures of the 20-in. BNL bubble chamber ⁽⁸⁾, and our proposed temperatures for big chambers are indicated by the dotted/dashed line.
- (18) Radiation length X^0 [cm] for various neon/hydrogen mixtures, with liquid temperature as the parameter.

Neon mole fraction	25	26	27	28	29	30	31	32	33	34	35	36	K
0.0	0.0647	0.0630	0.0612	0.0592	0.0569	0.0542	0.0510	0.0476	0.0900	--	--	--	
0.1	0.1264	0.1229	0.1191	0.1148	0.1102	0.1050	0.98						
0.2		0.188	0.182	0.176	0.169	0.161	0.151						
0.3			0.254	0.246	0.237	0.227	0.213						
0.4					0.314	0.302	0.287						
0.5					0.407	0.391	0.376						
0.6						0.498	0.482						
0.7						0.626	0.610						
0.8						0.772	0.755						
0.9				0.981	0.963	0.946	0.928						
0.95			1.098	1.080	1.060	1.042	1.025						
1.0	1.240	1.224	1.206	1.189	1.170	1.151	1.131	1.110	1.089	1.066	1.043	1.02	

Table 1

Measured densities ρ_L [g/cm³] of saturated liquid Ne-nH₂ mixtures at different temperatures T

Neon mole fraction	25	26	27	28	29	30	31	32	33	34	35	36	K
0.0	965	923	877	827	771	707	630	510	320	--	--	--	
0.1	692	661	627	588	545	496	435						
0.2		560	530	498	462	420	371						
0.3			468	443	412	376	335						
0.4					386	357	326						
0.5					368	349	323						
0.6						345	329						
0.7						361	349						
0.8						403	390						
0.9				499	484	469	452						
0.95			557	541	524	507	488						
1.0	628	613	596	580	562	544	526						

Table 2

Measured sound velocities c [m/s] of saturated liquid Ne-nH₂ mixtures at different temperatures T

Liquid mixture mole %	Temperature		Static pressure bar	Minimum pressure bar	Pressure drop bar	Piston stroke mm	$\Delta V/V$ %	Isentropic compressibility bar^{-1}	Remarks
	K	bar							
0/100	28.0 (27.7)*	6.0	7.0	3.6	3.4	28.0	0.98	$2.9 \cdot 10^{-3}$	
			7.0	3.8	3.2	25.0	0.87		
			7.0	4.1	2.9	22.0	0.76		
	29.0 (28.7)*	7.1	7.7	4.7	3.0	28.5	0.99	$3.3 \cdot 10^{-3}$	
			7.7	5.0	2.7	25.5	0.88		
			7.7	5.3	2.4	22.0	0.76		
	29.5 (29.3)*	7.7	7.9	5.3	2.6	28.0	0.98	$3.7 \cdot 10^{-3}$	
			7.9	5.6	2.3	24.5	0.85		
			7.9	6.0	1.8	20.5	0.71		
31.9/68.1	28.0	6.1	7.0	3.8	3.2	28.5	0.99		partial phase separ.
			7.0	3.8	3.2	25.0	0.87		
	28.5	6.7	8.0	4.4	3.7	25.5	0.88	$2.0 \cdot 10^{-3}$	
			8.0	4.7	3.3	23.0	0.80		
			8.0	5.0	3.0	20.6	0.72		
	28.95	7.2	8.5	5.0	3.5	25.0	0.87	$2.5 \cdot 10^{-3}$	
			8.5	5.4	3.0	22.5	0.78		
			8.5	5.9	2.6	19.8	0.69		

Table 3

Operating conditions of the DESY bubble chamber

() * Average values after correction for adiabatic temperature drop

Liquid mixture mole %	Temperature		Static pressure bar	Minimum pressure bar	Pressure drop bar	Piston stroke mm	$\Delta V/V$ %	Isentropic compressibility bar^{-1}	Remarks
	K	bar							
53.8/46.2	28.8	6.7	7.2	5.2	2.0	14.5	0.49		phase separation
	29.0	7.0	8.4	4.7	3.7	20.2	0.70	$1.9 \cdot 10^{-3}$	
			8.4	5.1	3.3	17.3	0.60		
			8.4	5.5	2.9	14.2	0.49		
83.8/16.2	28.95	6.8	8.1	2.0	6.1	14.0	0.49	$0.8 \cdot 10^{-3}$	
			8.1	3.6	4.5	11.5	0.40		
			8.1	4.3	3.8	9.4	0.33		
	29.45	7.2	8.4	3.2	5.2	18.2	0.63	$1.2 \cdot 10^{-3}$	
			8.4	3.8	4.6	15.5	0.54		
			8.4	4.4	4.0	12.8	0.45		
86.6/13.4	28.5	6.3	8.1	2.2	5.9	11.6	0.40	--	no PV-diagram
			8.1	2.5	5.5	8.9	0.31		
			8.1	3.0	5.1	7.9	0.27		
	29.4	7.1	8.3	2.7	5.6	9.0	0.31	--	no PV-diagram
			8.3	3.1	5.2	8.4	0.29		
			8.3	3.5	4.8	7.6	0.26		

Table 3 (contd.)

Operating conditions of the DESY bubble chamber

Liquid mixture mole %	Temperature		Static pressure bar	Minimum pressure bar	Pressure drop bar	Piston stroke mm	$\Delta V/V$ %	Isentropic compressibility bar^{-1}	Remarks
	K	bar							
92.3/7.7	28.0	5.5	7.2	1.2	6.0	7.1	0.25	--	no PV-diagram not track sensitive
			7.2	1.8	5.4	6.4	0.22		
	29.5	6.2	8.0	2.0	6.0	10.0	0.35	$0.45 \cdot 10^{-3}$	
			8.0	2.4	5.6	7.9	0.27		
			8.0	2.8	5.2	7.2	0.25		
	30.0	6.5	8.2	2.0	6.2	9.9	0.35	$0.44 \cdot 10^{-3}$	
			8.2	2.3	5.9	8.7	0.30		
			8.2	2.5	5.7	8.0	0.28		
	96.7/3.3	29.0	4.2	6.5	0.9	5.6	7.0	0.24	$0.32 \cdot 10^{-3}$
30.0		4.7	6.7	1.4	5.3	8.2	0.29	$0.37 \cdot 10^{-3}$	
31.0		5.4	7.5	1.6	5.9	9.4	0.33	$0.42 \cdot 10^{-3}$	
			7.5	2.0	5.5	6.8	0.23		
32.0	6.2	8.0	2.1	5.9	9.9	0.34	$0.46 \cdot 10^{-3}$		
		8.0	2.5	5.5	8.1	0.28			
100/0	34.5	5.9	7.2	2.1	5.1	8.8	0.31	$0.48 \cdot 10^{-3}$	
	34.9	6.4	7.3	2.3	5.0	12.0	0.42	$0.54 \cdot 10^{-3}$	
			7.2	2.6	4.6	8.7	0.30		
7.3			3.6	3.7	6.0	0.26			

- 25 -

Table 3 (contd.)

Operating conditions of the DESY bubble chamber

	Condition 1 20/80 mole % neon/hydrogen	Condition 2 20/80 mole % neon/hydrogen	Comparison hydrogen	
Liquid temperature T	26.5	26.5	25.3	K
Expanded pressure P _{min}	1.9	2.8	1.6	bar
Static pressure P _s	5.5	5.5	4.5	bar
Cycle duration L	80	80	55	ms
Expansion ratio ΔV/V	1.0	0.7	0.7	%
Sound velocity c	545	545	955	m/s
Isentropic compressibility β	2.0	2.0	1.8	10 ⁻³ bar ⁻¹
Liquid density ρ _L	0.185	0.185	0.064	g/cm ³
Bubble growth constant A	0.4	0.19	0.4	cm/s ^{1/2}
Bubble density b	50	10	10	cm ⁻¹

Table 4

Proposed working conditions for a 20/80 mole percent neon/hydrogen mixture and for comparison an optimum condition for pure hydrogen

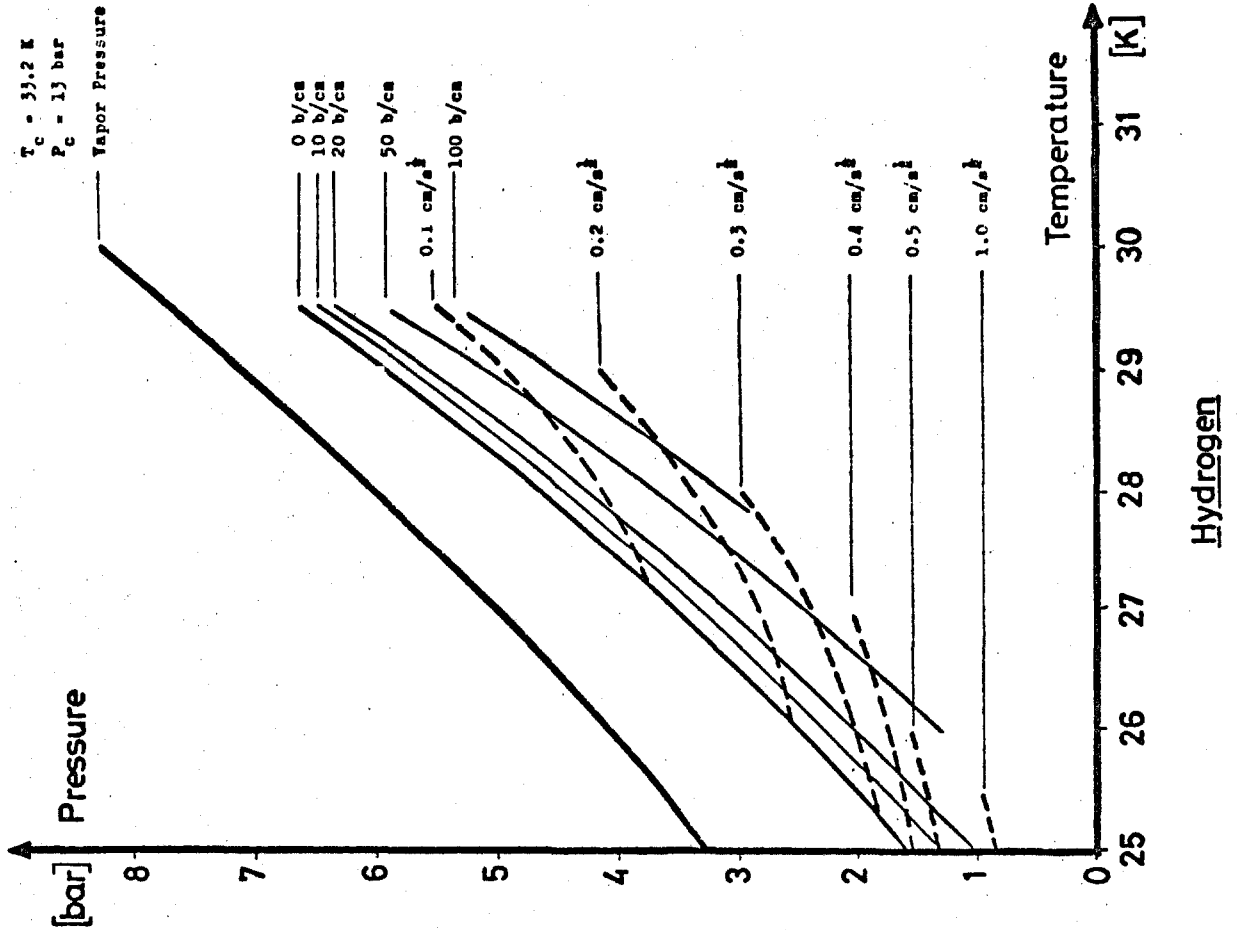


FIG.2

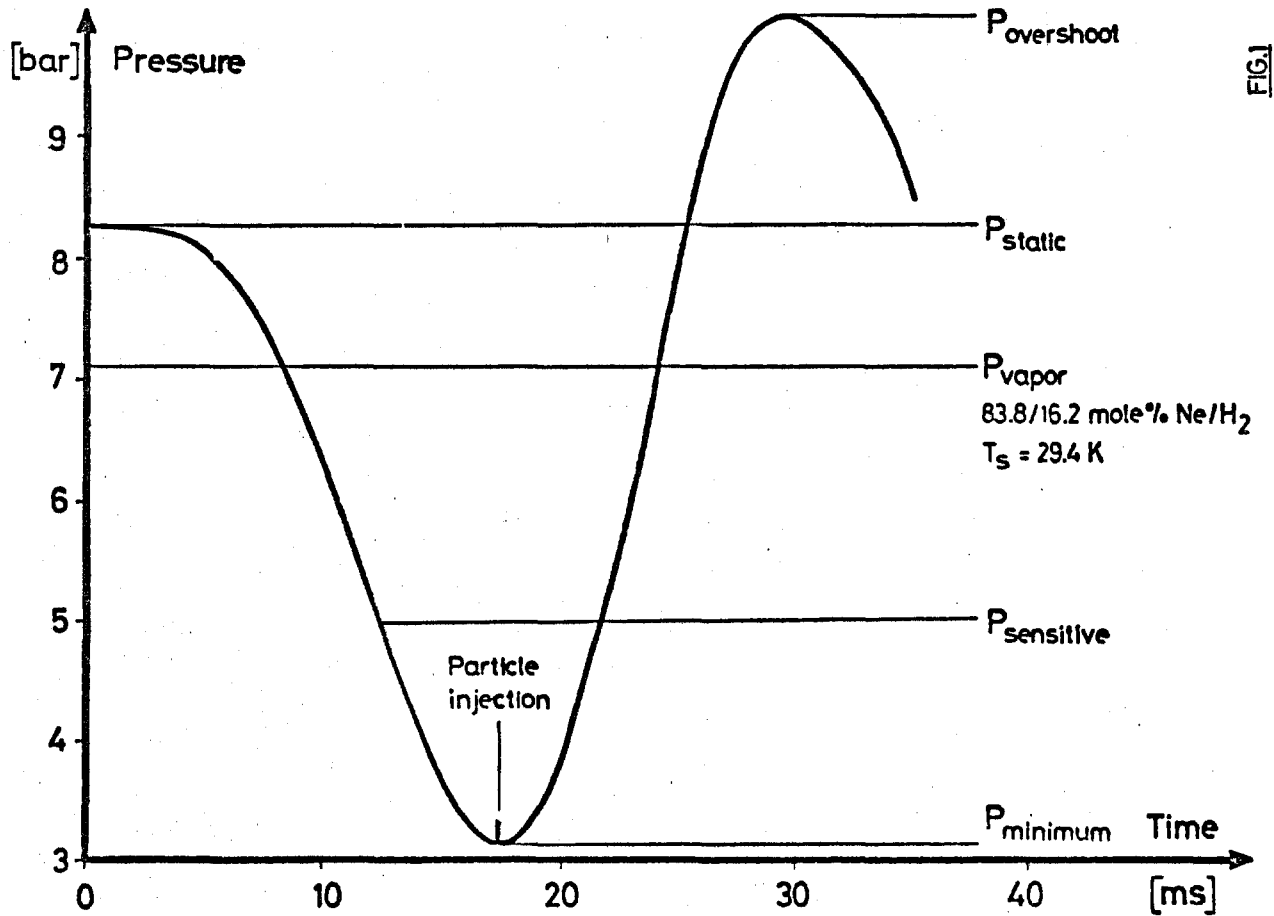
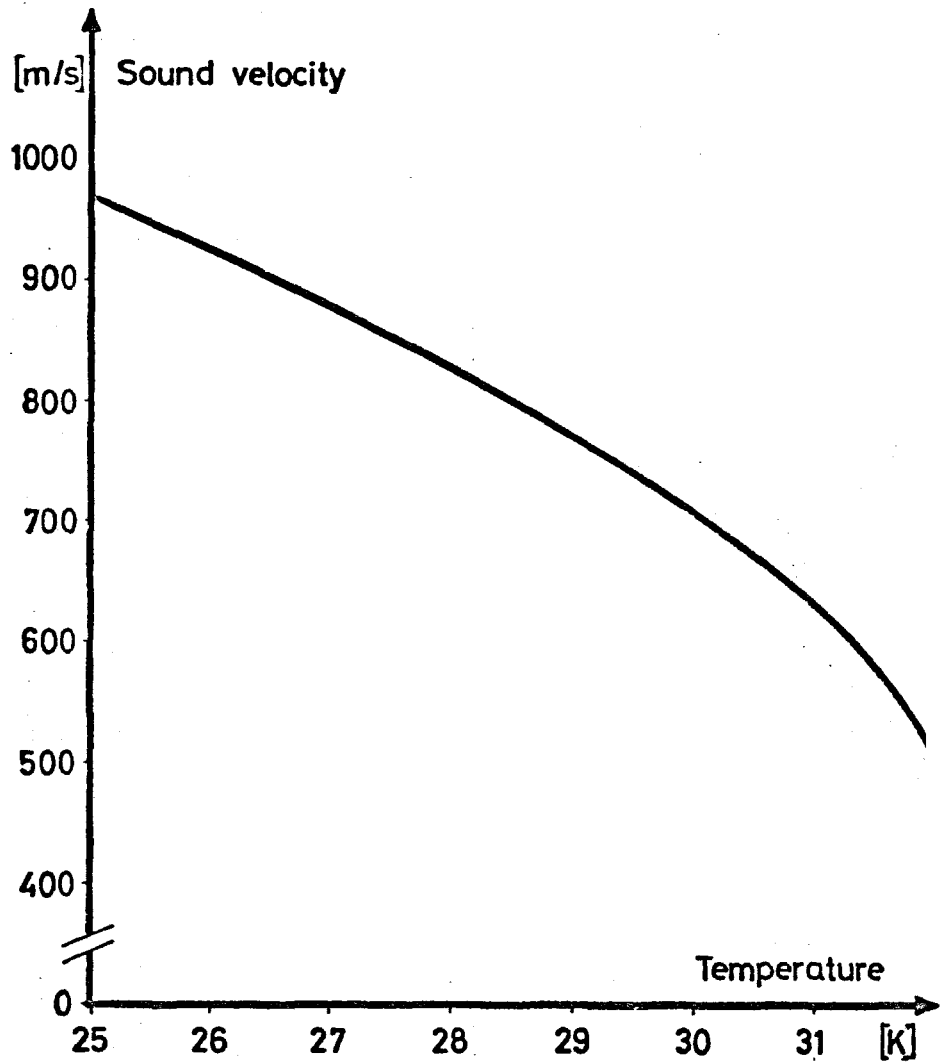
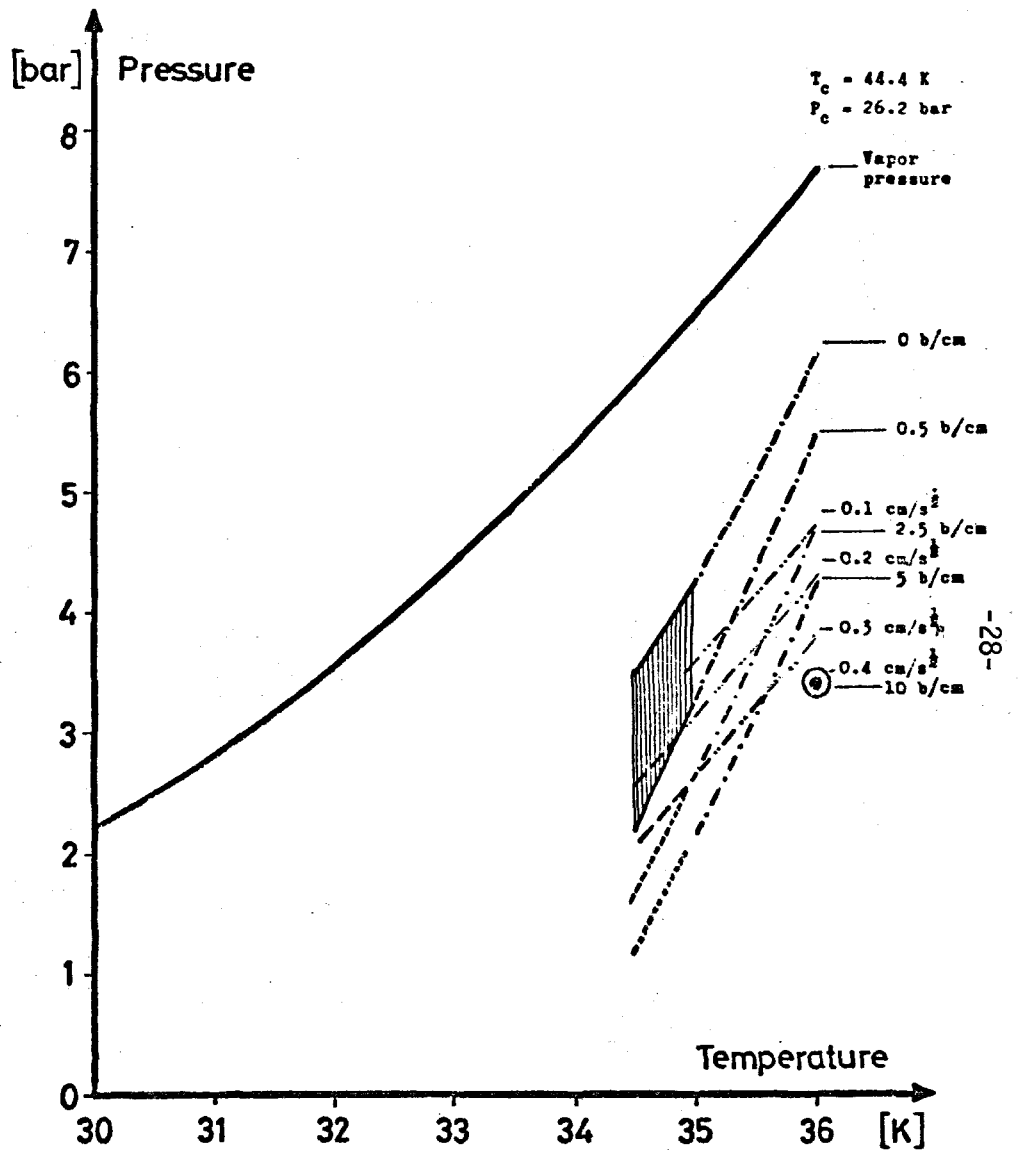


FIG.1



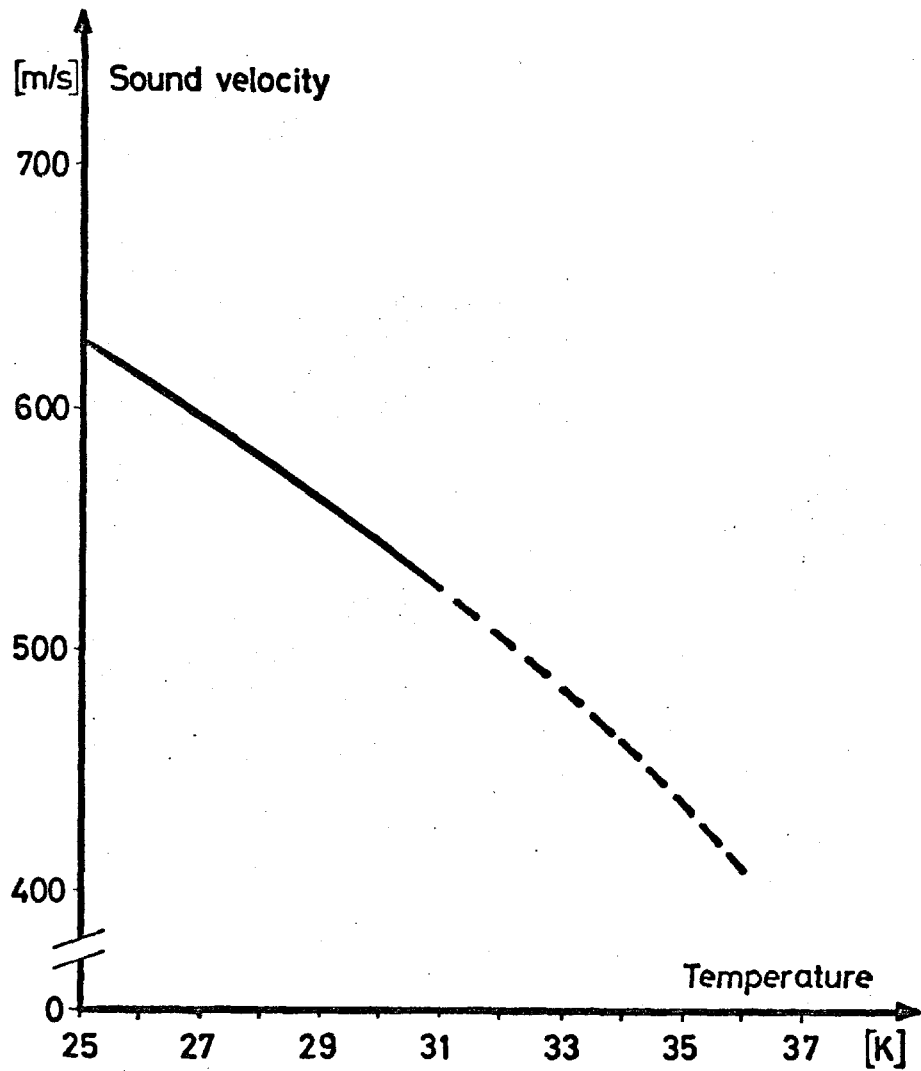
Hydrogen

FIG. 3



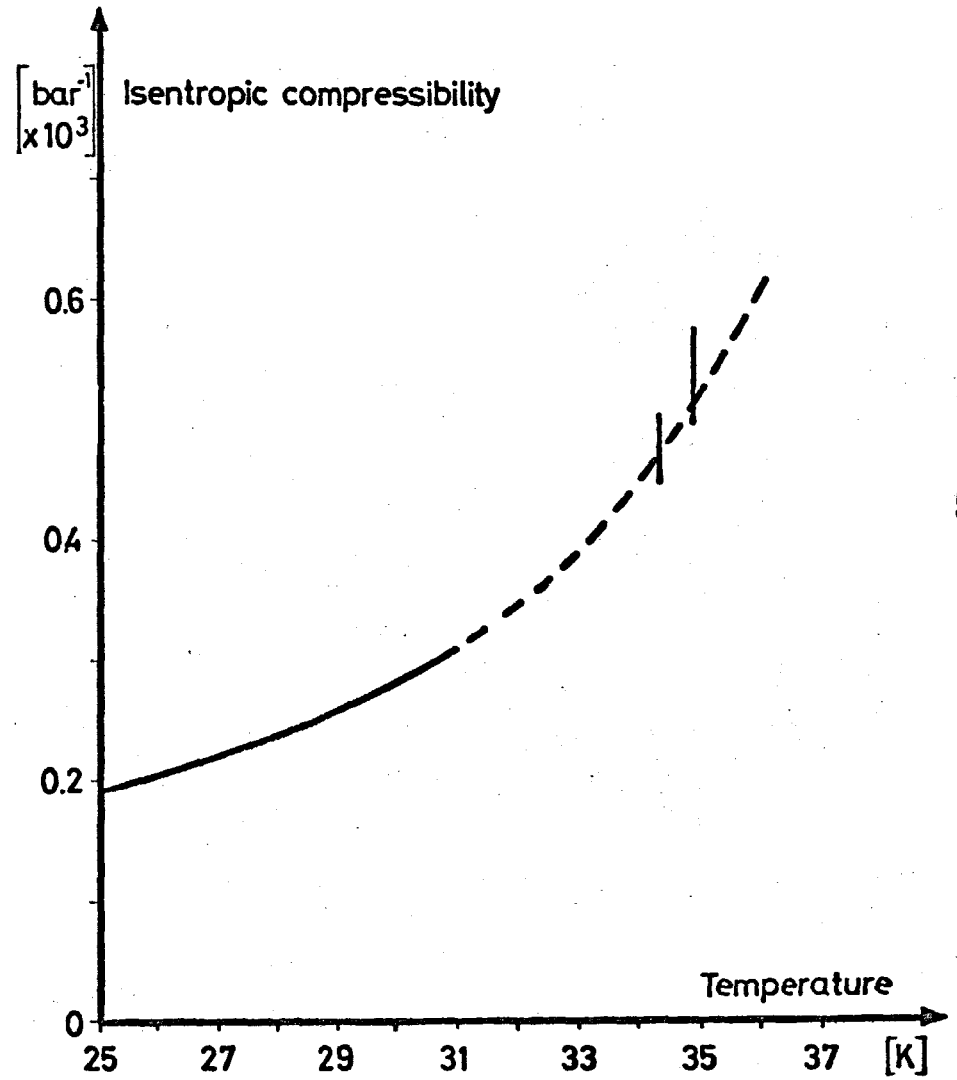
Neon

FIG. 4



Neon

FIG.5



Neon

FIG.6

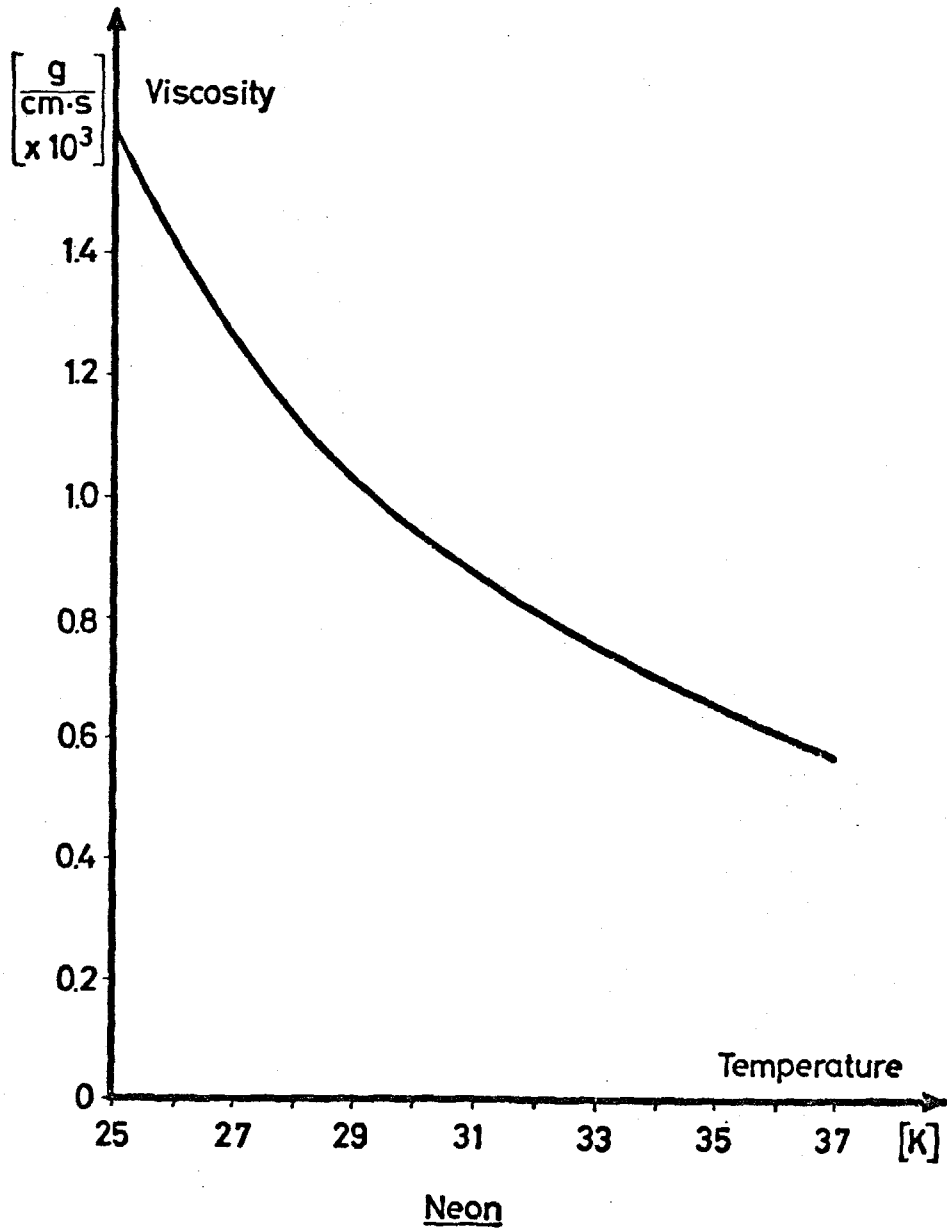
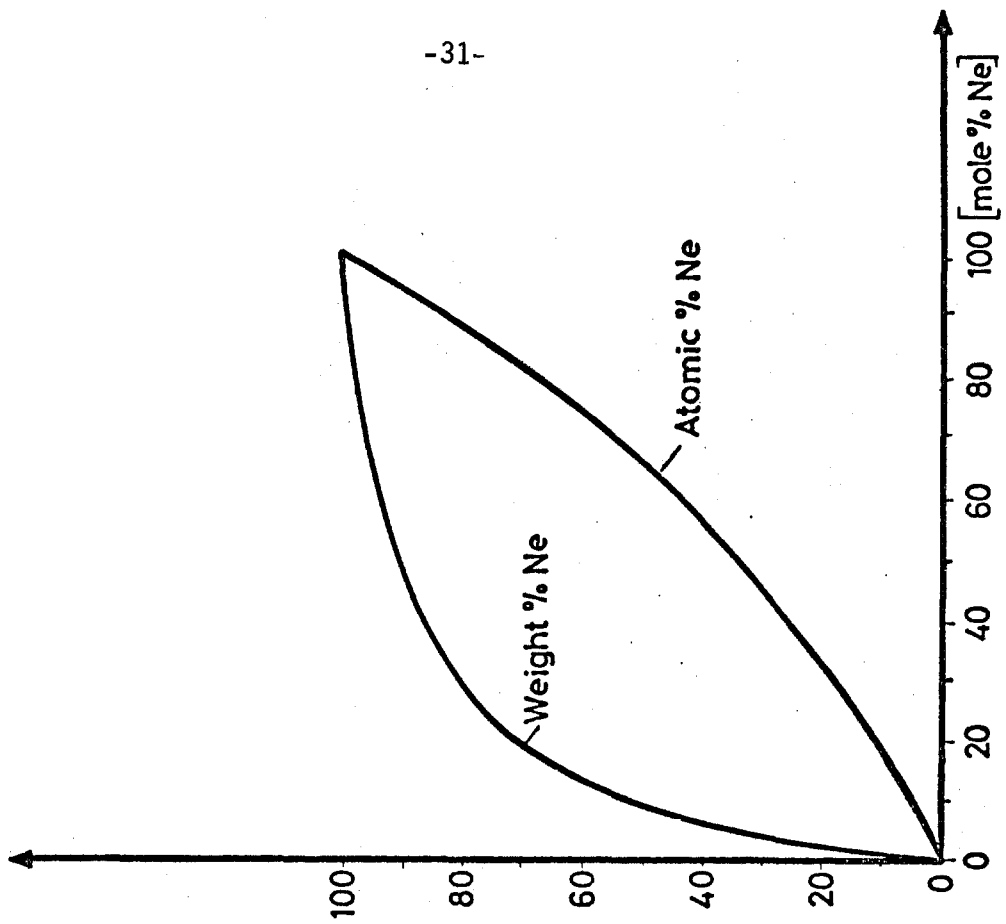


FIG.7



FIG.8



Neon/hydrogen mixtures

FIG.10

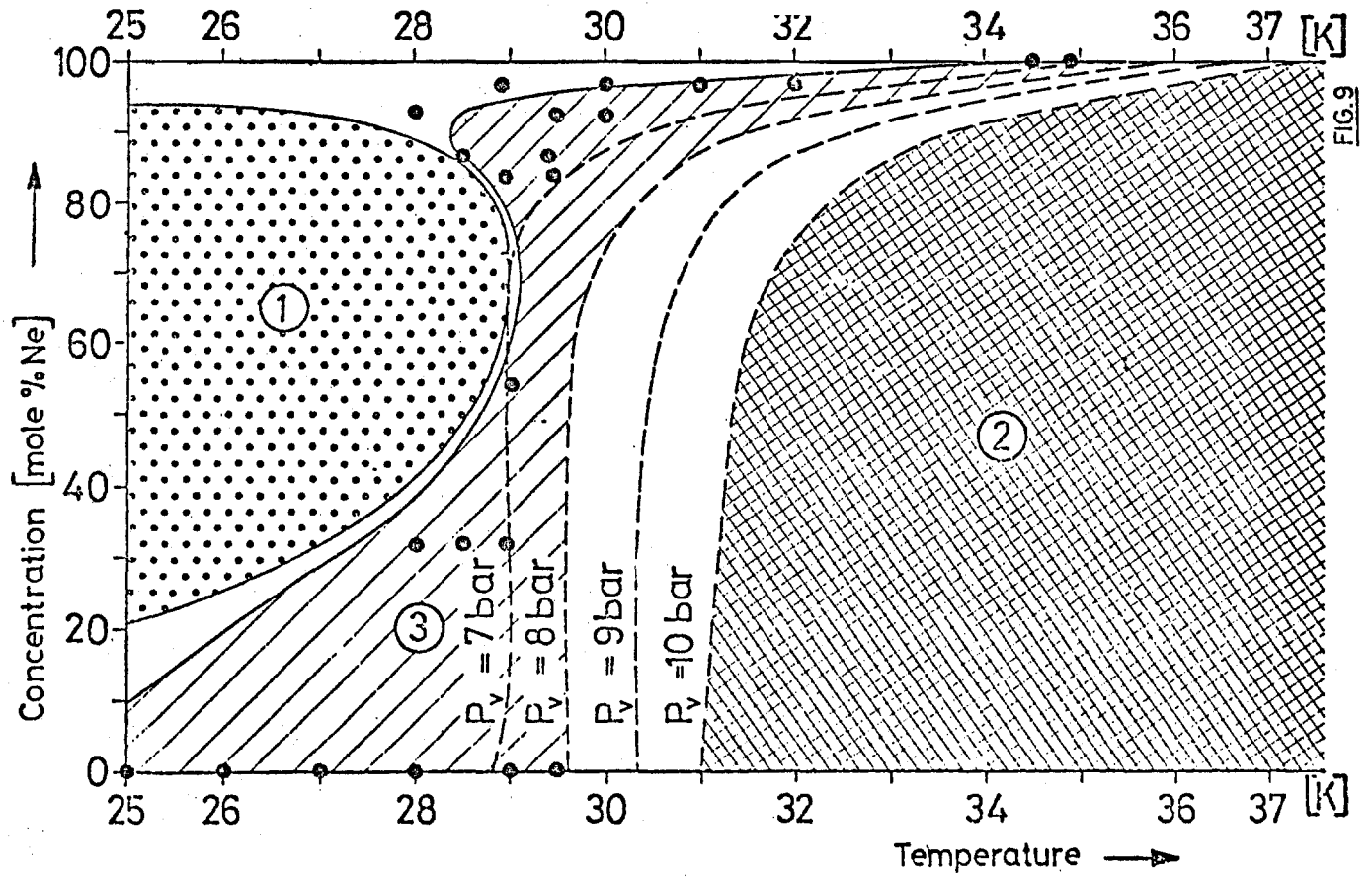
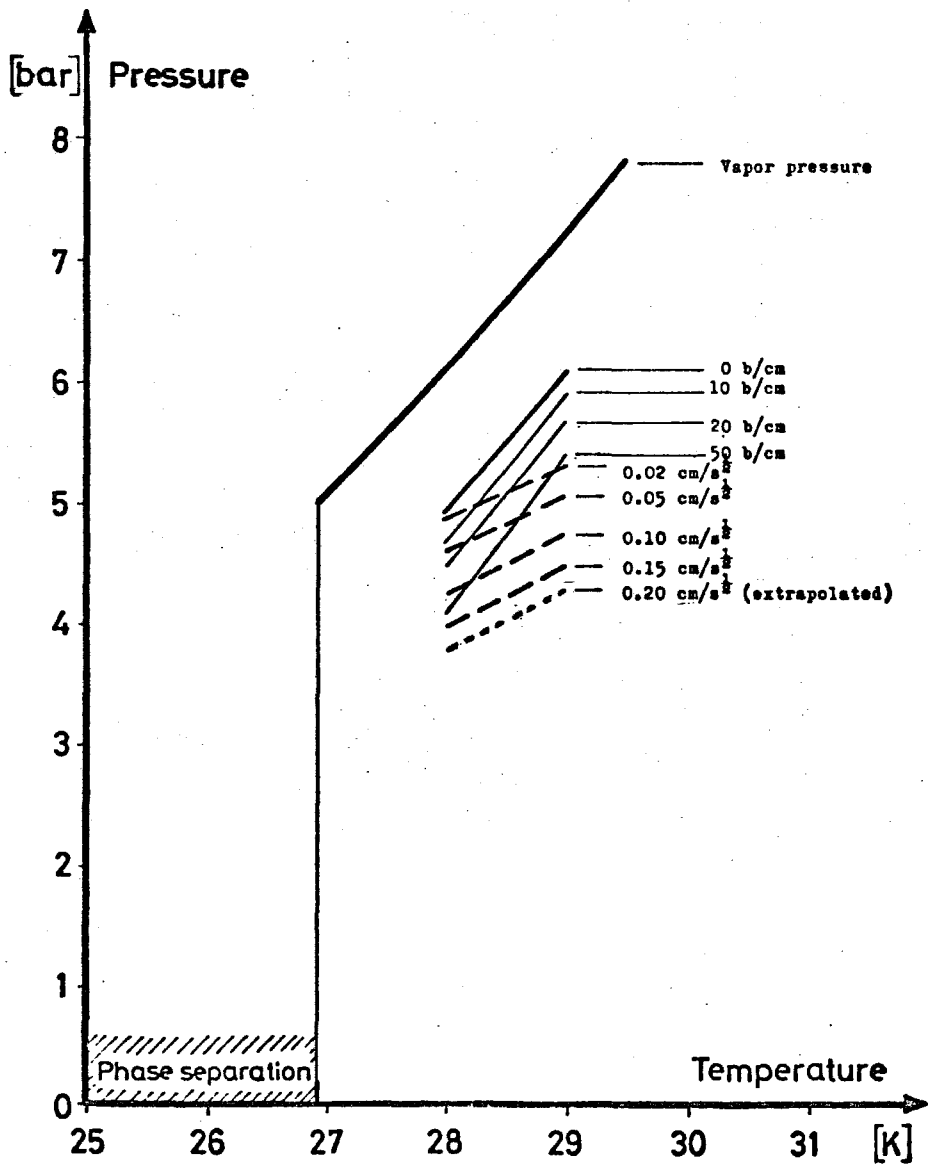
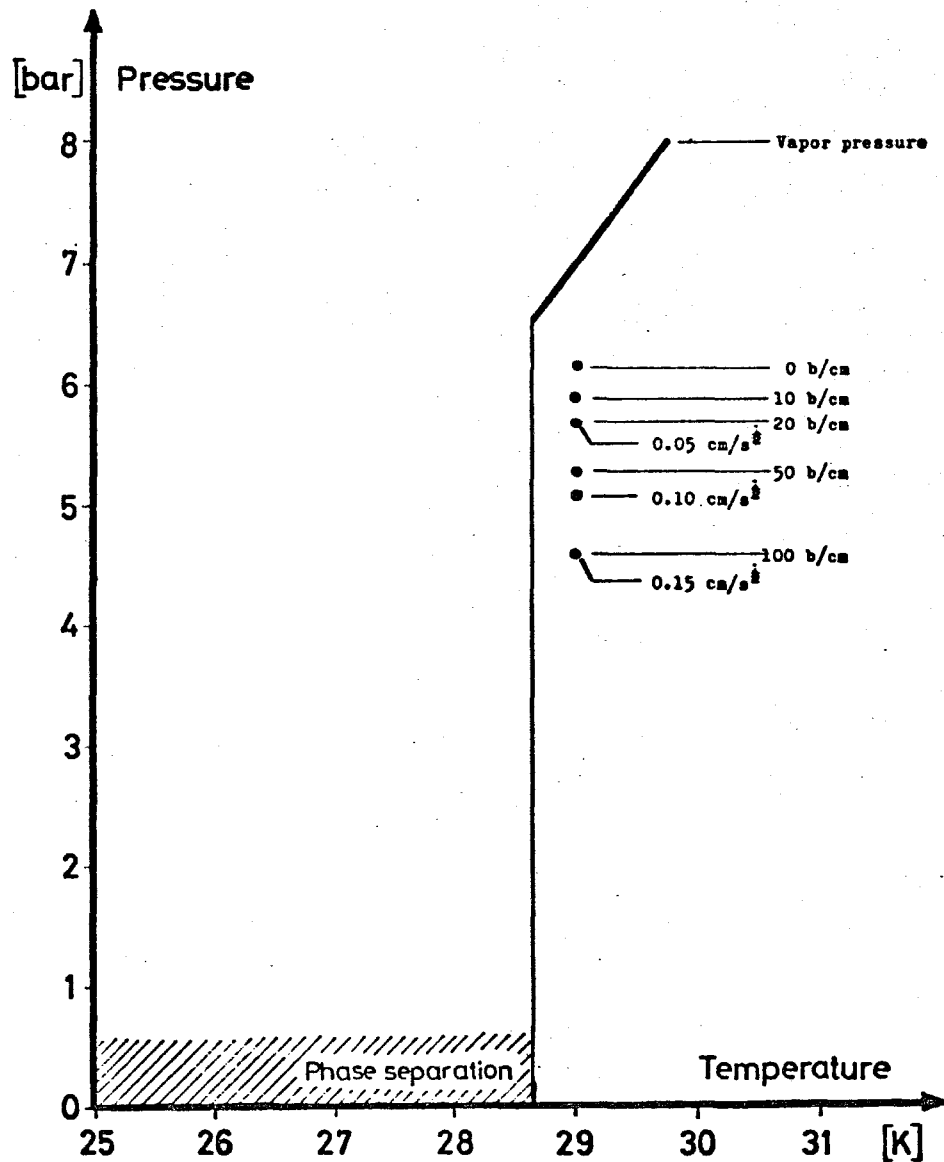


FIG.9



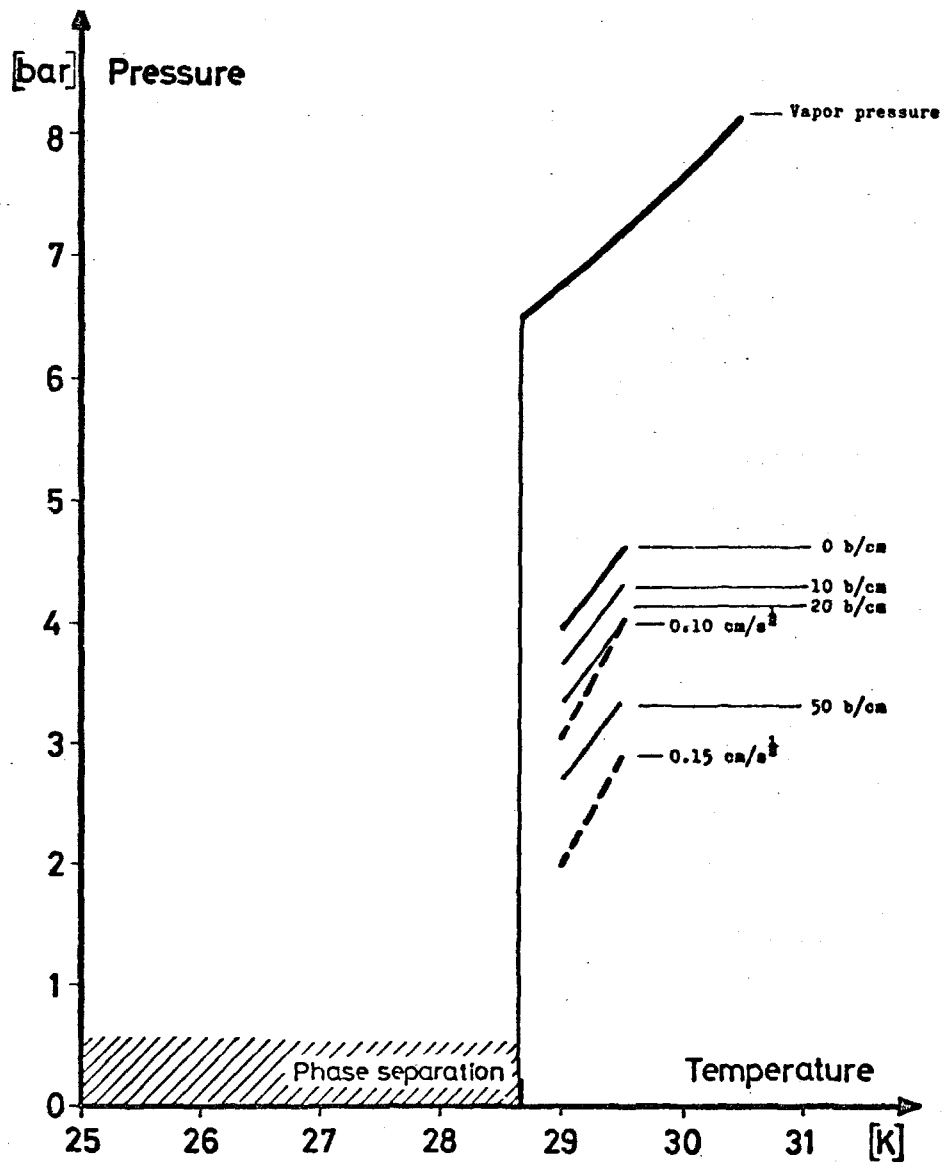
31.9/68.1 mole % Ne/H₂

FIG. 11



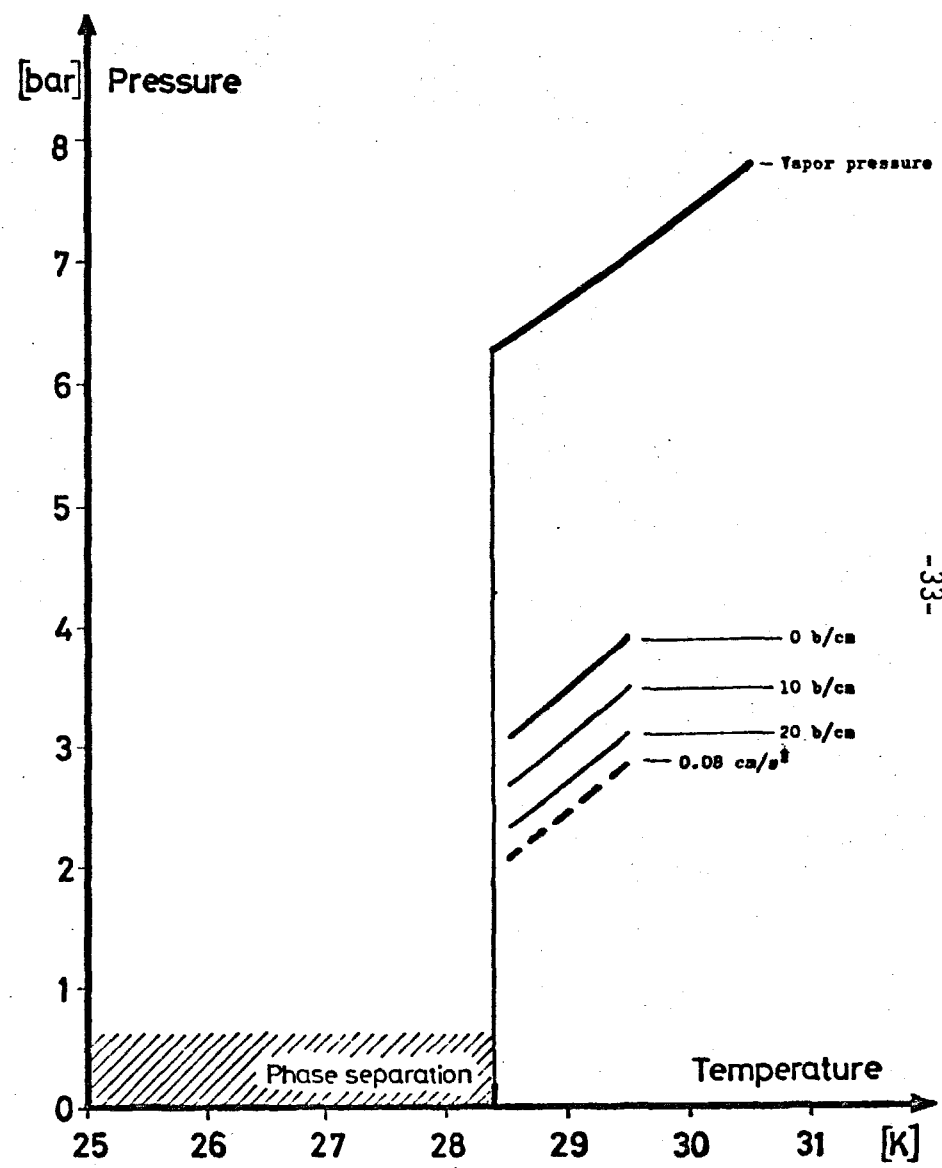
53.8/46.2 mole % Ne/H₂

FIG. 12



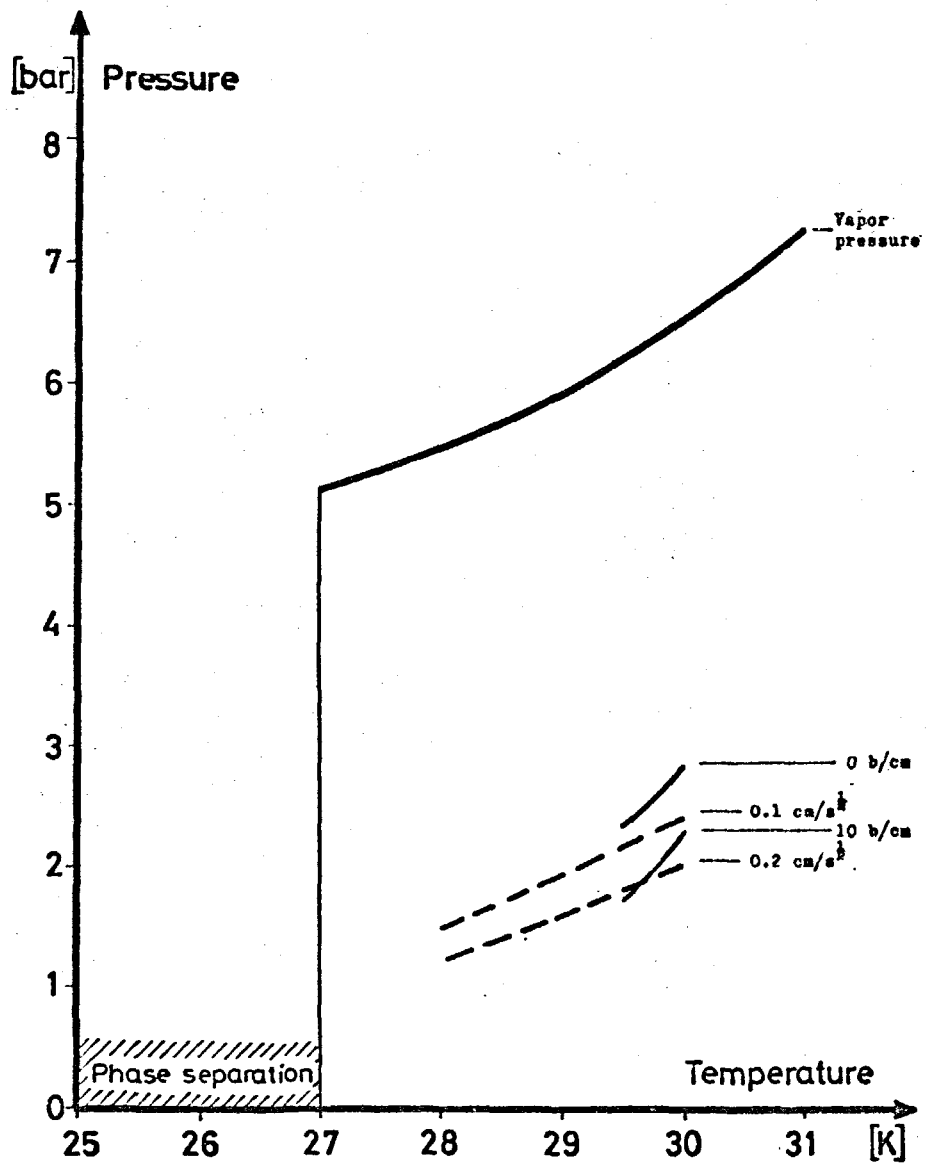
83.8/16.2 mole % Ne/H₂

FIG. 13



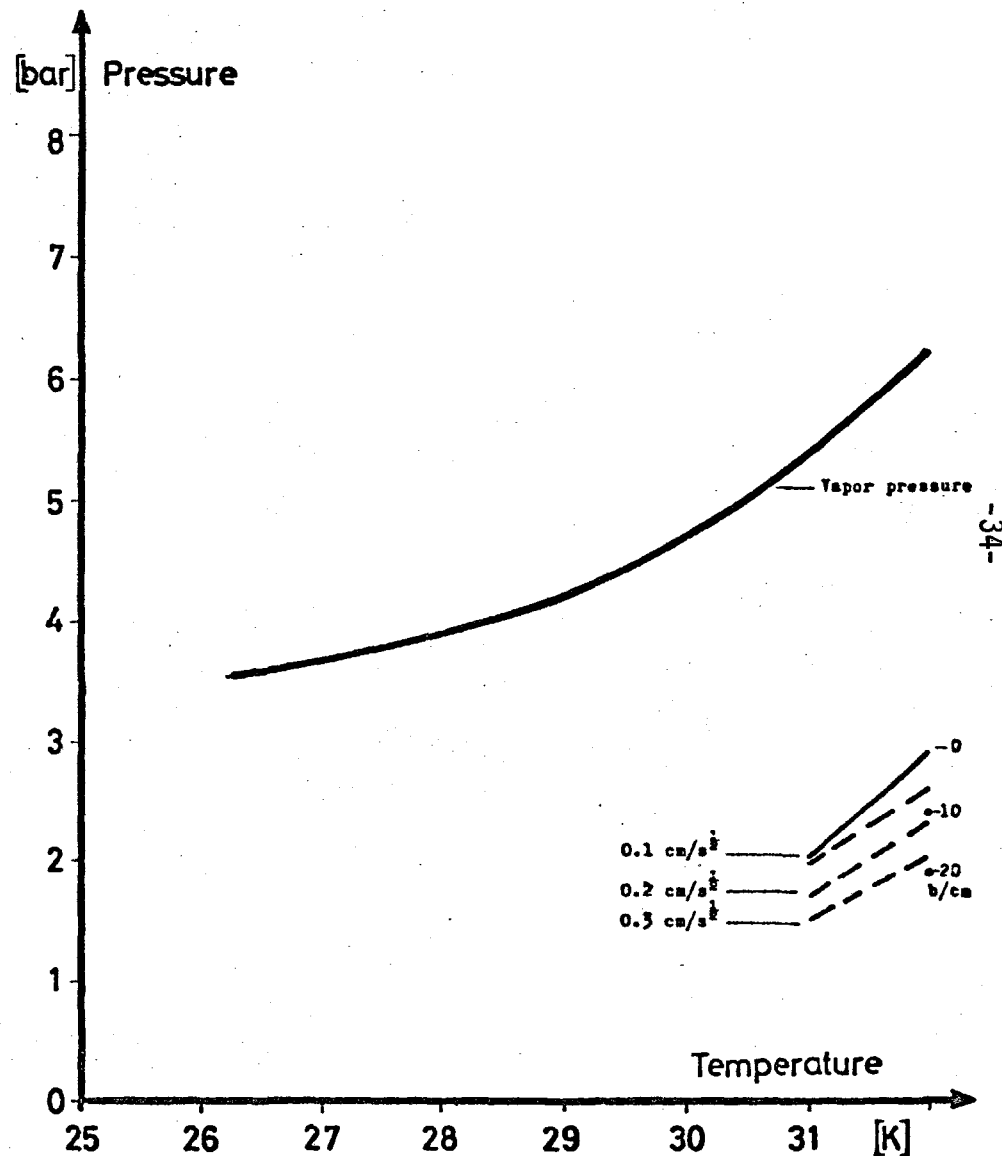
86.6/13.4 mole % Ne/H₂

FIG. 14



92.3/7.7 mole % Ne/H₂

FIG. 15



96.7/3.3 mole % Ne/H₂

FIG. 16

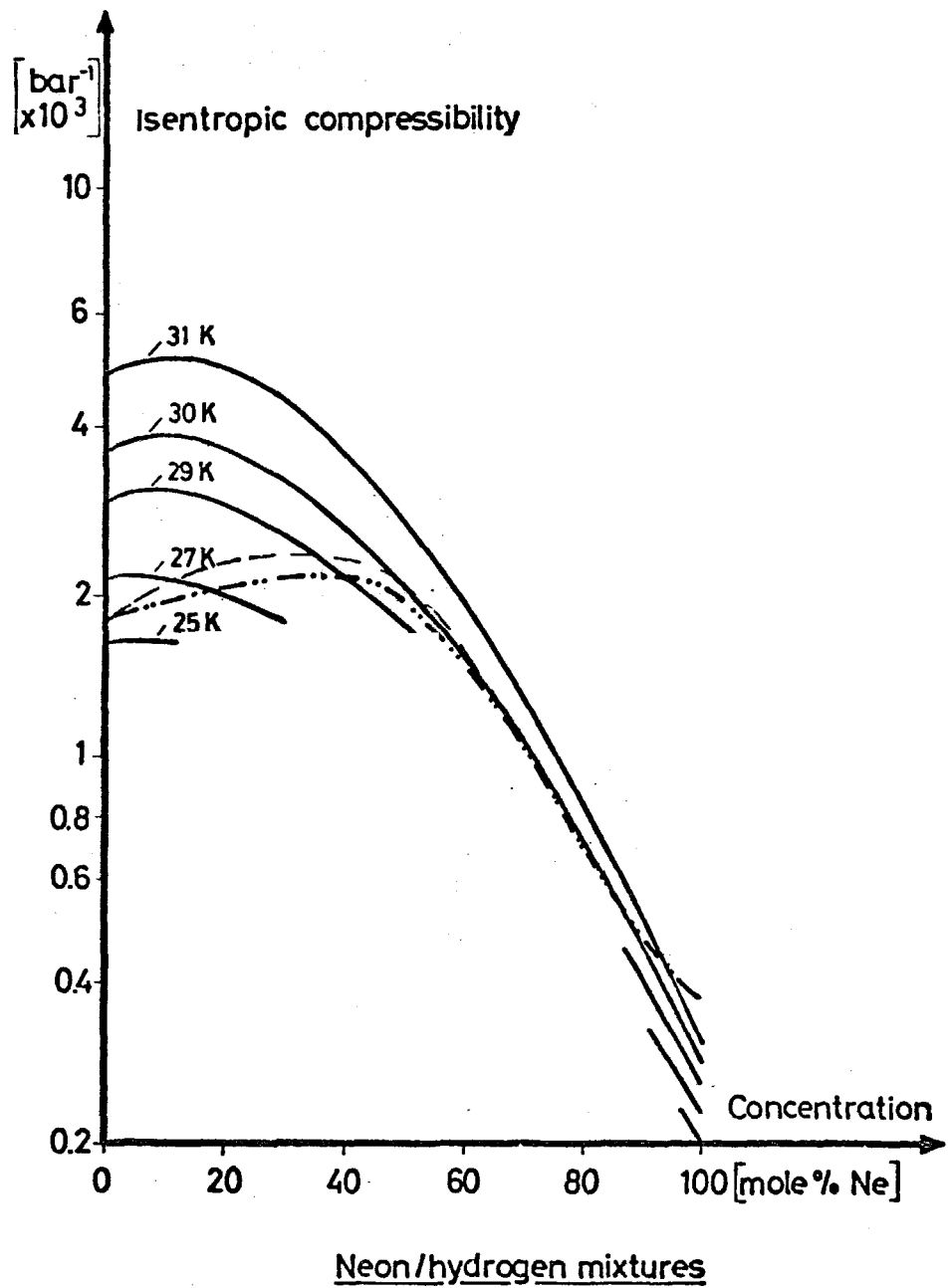


FIG. 17

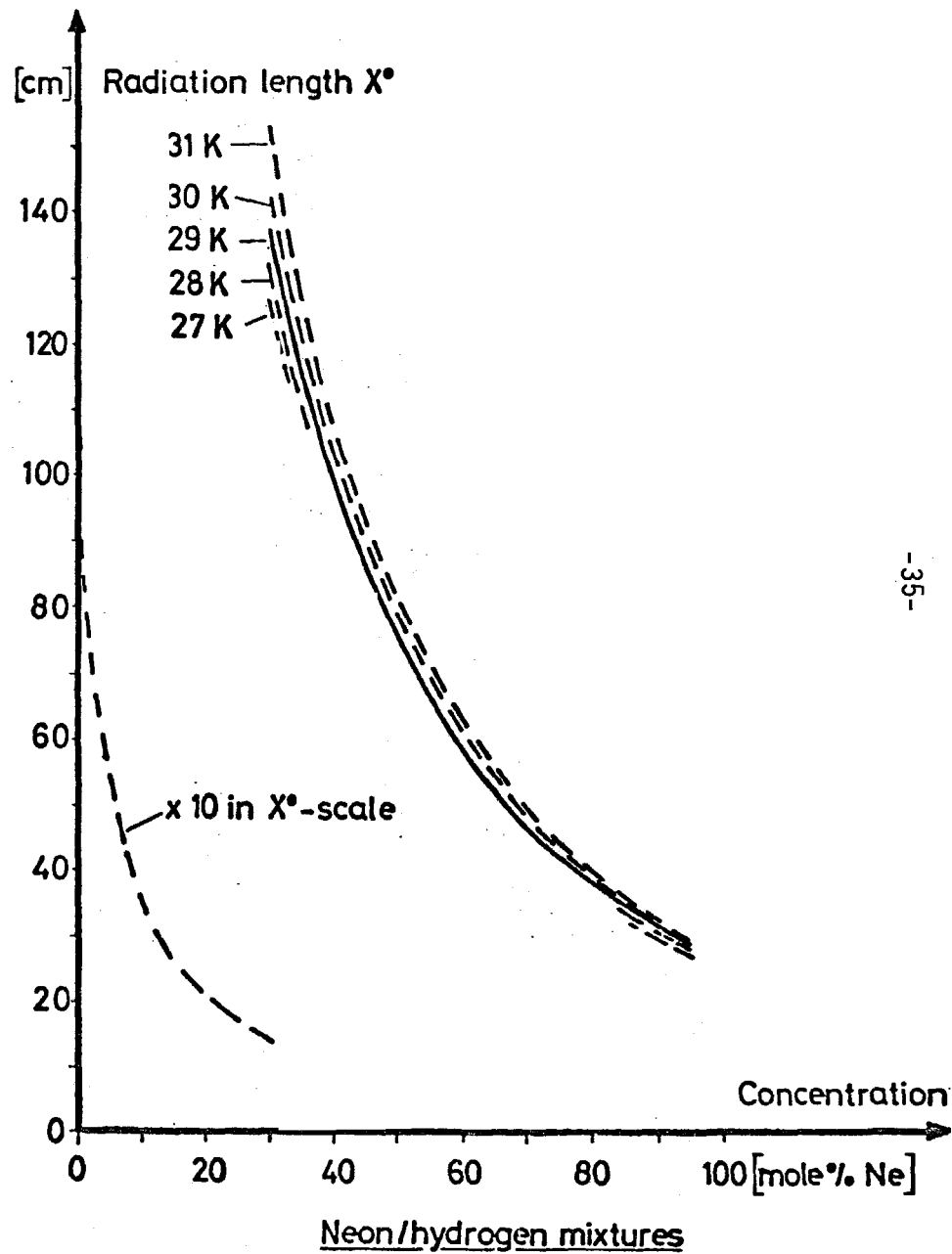


FIG. 18